Journal of Visualization, Vol. 12, No. 3 (2009) 195-202

Regular Paper

Visualizing Shear Stress in Görtler Vortex Flow

Tandiono*, Winoto, S. H.* and Shah, D. A.*

* Department of Mechanical Engineering, National University of Singapore, 9 Engineering Drive 1, Singapore 117576, Singapore, E-mail: mpewinot@nus.edu.sg

Received 10 October 2008
Revised 29 January 2009

Abstract : Shear stress distributions were obtained from velocity measurements in a concave surface boundary layer flow in the presence of Görtler vortices by means of a single hot-wire probe for several streamwise (x) locations. A set of vertical wires of 0.20 mm diameter were positioned at a distance of 10 mm upstream from the leading edge of a concave surface of radius of curvature R = 1.0 m to pre-set the wavelength of the vortices so to obtain the most amplified wavelength Görtler vortices. Consequently, the wavelength of the vortices was set equal to the wire spacing and preserved downstream. In addition to the high shear regions near the wall, one positive peak at the head of the mushroom-like structures and two relatively weak negative peaks at the vicinity of the low-speed streaks are found in the iso-$\partial u/\partial y$ contours. They are believed to be related to the formation of the inflectional point in the velocity profile across boundary layer. The occurrence of the inflection points in the spanwise distributions of streamwise velocity component u is associated with the appearance of the second peak of the $\partial u/\partial z$ shear near the boundary layer edge. The nonlinear effect of Görtler instability is to increase the wall shear stress, and further enhancement beyond the turbulent values is due to the presence of secondary instability.

Keywords : Görtler vortices, Concave surface, Shear stress, Boundary layer flow.

1. Introduction

Concave surface boundary layer flows can be found in many fluid engineering applications, such as on turbine blades and airfoils. The main feature of such boundary layer flows is the presence of streamwise counter-rotating Görtler vortices (Görtler, 1940), due to the imbalance between the radial pressure gradient and the centrifugal force in the boundary layer flow. These vortices cause sinusoidal variation in the boundary layer thickness in the spanwise direction. Two distinct regions known as “upwash” and “downwash” can be identified either by flow visualization or from streamwise velocity measurement in the spanwise (z) direction. The upwash refers to the region where low momentum fluid moves away from concave surface resulting in lower shear stress region and thicker boundary layer, while at the downwash region high momentum fluid moves towards the surface resulting in higher shear stress region and thinner boundary layer.

The vortices in concave surface boundary layer flow will be amplified downstream resulting in a three-dimensional boundary layer that is receptive to secondary instability when the flow field becomes sufficiently nonlinear. Two distinct modes, namely sinuous and varicose modes, of the secondary instability were found numerically by Hall and Horseman (1991). These modes are related to the appearance of the intense shear regions in the upwash region of iso-$\partial u/\partial y$ and iso-$\partial u/\partial z$ contours. Yu and Liu (1994) showed that the sinuous and varicose modes were mainly attributed to the Reynolds stress conversion mechanism associated with $\partial u/\partial y$ and $\partial u/\partial z$ shear, respectively. It is therefore important to present the shear stress distributions, in addition to the

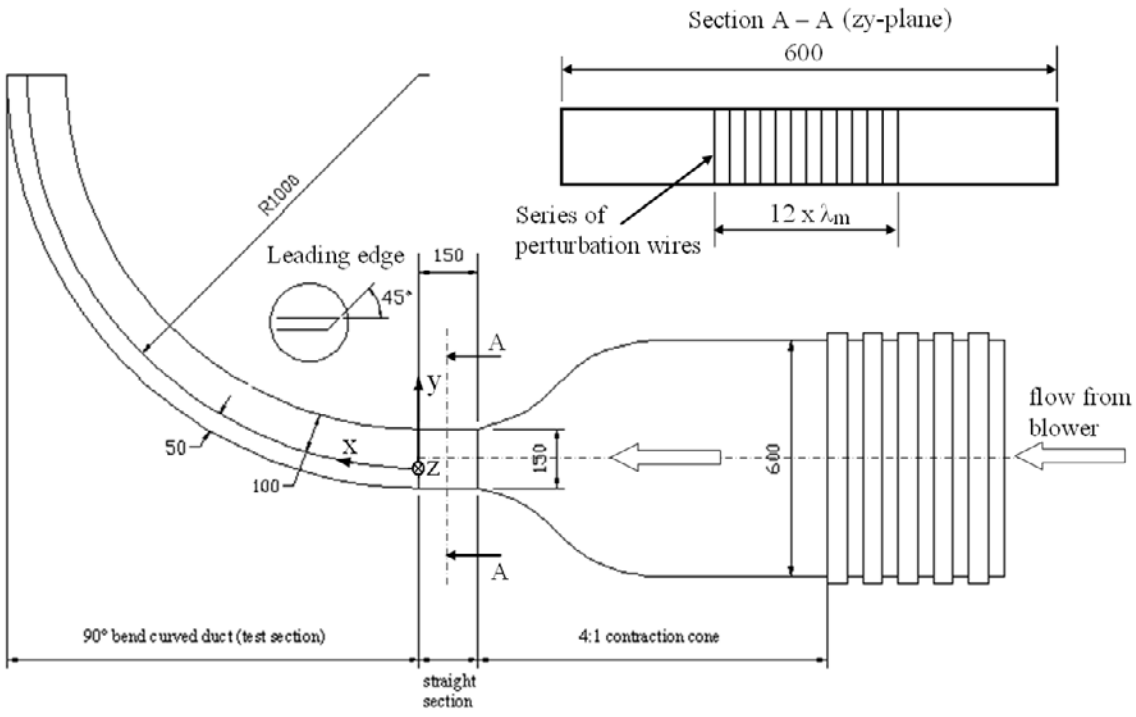

Fig. 1. Schematic of experimental set-up (all dimensions are in mm)

mean streamwise velocity distributions, obtained from experiments since only few experimental data are available in the literature.

Many flow visualizations of Görtler vortices have been performed for various flow conditions in concave surface boundary layers. Earlier experiments were conducted for naturally developed Görtler vortices, such as Wortmann (1969), Bippes and Görtler (1972), Winoto and Crane (1980), Swearingen and Blacwelder (1987), and Petitjeans et al. (1997). A major drawback of naturally developed Görtler vortices is that the resulting vortices possess non-uniform wavelengths which cause difficulty and subjectivity in studying the behavior of the vortices. To overcome this problem, the wavelength of Görtler vortices can be pre-set or "forced" by introducing orderly disturbances prior to the leading edge of the concave surface. Peerhossani and Bahri (1998) used a series of thin vertical wires placed prior and perpendicular to the concave surface leading edge. This method was also adopted by Ajakh et al. (1999), Mitsudharmadi et al. (2004), and Winoto et al. (2005) since it could effectively generate Görtler vortices with uniform wavelength equal to the pre-set spanwise spacing of the thin perturbation wires.

The aim of this work is to experimentally study the distributions of shear stress in concave surface boundary layer flow in the presence of pre-set wavelength Görtler vortices. The mean streamwise velocity and shear stress distributions were visualized by plotting the contours from the velocity data obtained from hot-wire anemometer measurement.

2. Details of Experiment

The experimental setup (Fig. 1) and the instrumentation system have been previously described by Tandiono et al. (2008). However, a brief description will be given for the convenience of the readers.

The experiments were conducted in a 90° curved plexiglass test section connected to a low speed, blow down type wind tunnel. A concave surface of radius of curvature R = 1.0 m is mounted inside the curved test section by means of slots at the test section side walls at a distance of 0.05 m from the bottom surface. The distance between the concave surface and its top cover is 0.10 m. A series of vertical perturbation wires of 0.2 mm diameter are placed at 10 mm prior and perpendicular to the concave surface leading edge to pre-set the wavelength of Görtler vortices. The

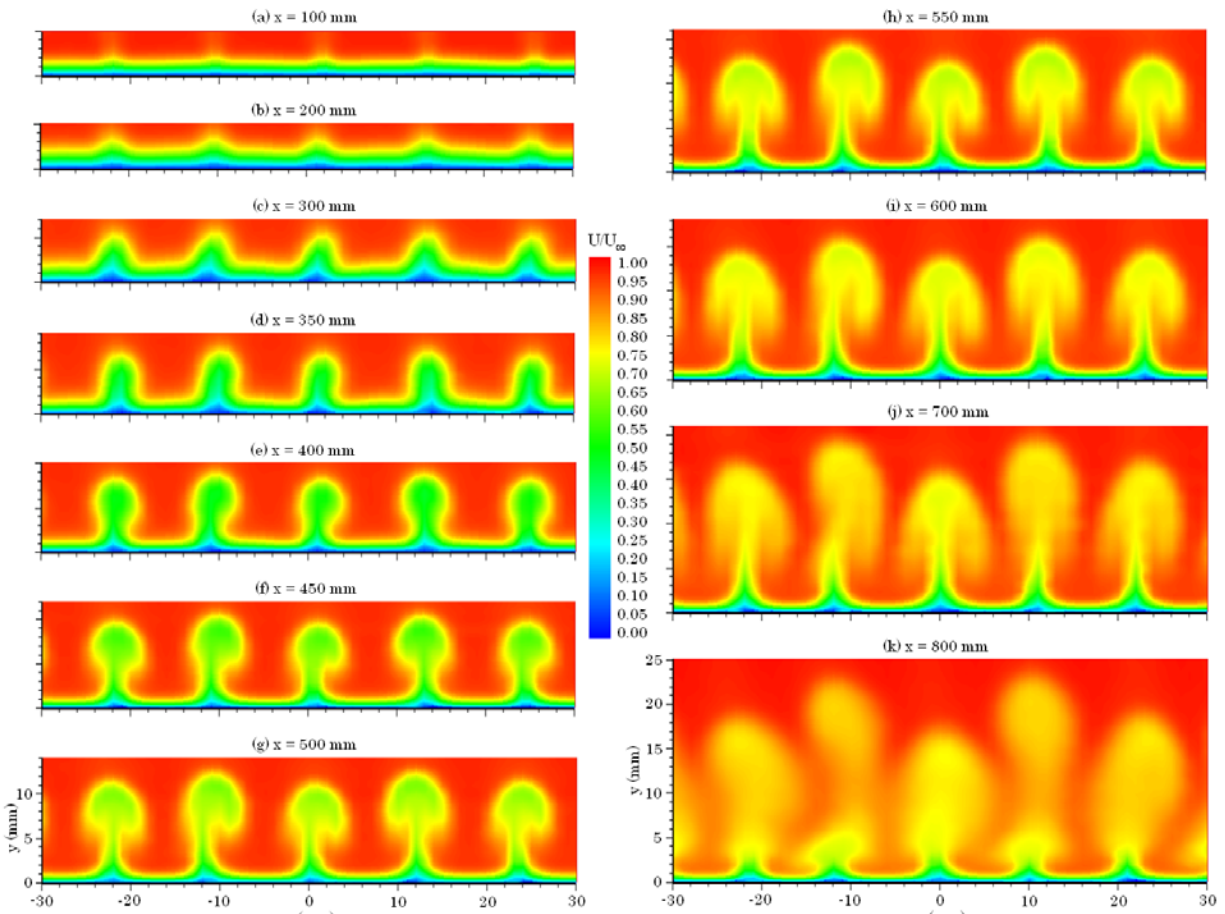

Fig. 2. Mean streamwise velocity (u/U_∞) contours on y-z plane for several streamwise (x) locations

free-stream velocity U_∞ is set at 2.85 m/s and the spanwise spacing between wires at 12 mm so the wavelength parameter Λ, which is defined as:

$$\Lambda = \frac{U_\infty \lambda_m}{\nu}\sqrt{\frac{\lambda_m}{R}} \tag{1}$$

is equal to 249. This value corresponds to the most amplified wavelength λ_m of Görtler vortices predicted by Görtler vortex stability diagram that is in the range of 220-270 (Luchini and Bottaro, 1998), where ν is the fluid kinematic viscosity and R the radius of curvature of the concave surface. The free-stream turbulence levels in the test section are less than 0.45% for U_∞ of 1.0 to 4.0 m/s.

A single hot-wire probe of special design for boundary layer measurement with a 5 µm diameter and 1 mm long tungsten wire was used to obtain mean and fluctuating streamwise velocity data. A Pitot-static tube connected to a pressure transducer and a *T*-type thermocouple were placed in the free-stream region and moved together with the hot-wire probe. They are used to monitor the free-stream velocity and temperature respectively, and to calibrate the CTA system. The measurement process (including data acquisition) and the traversing mechanism (with an accuracy of ±0.005 mm) are automatically controlled by a personal computer. The hot-wire signal was low-pass filtered at 3000 Hz and sampled at 6000 Hz for 21 seconds. Calibration checks were regularly performed to ensure that the drift is within an acceptable range of ±1%, otherwise the data obtained were rejected.

Measurements of the streamwise velocity component were carried out at several streamwise (x) locations. Five pairs of vortices were identified by the hot-wire measurement with 1.0 mm traversing step along the spanwise (z) direction and 0.5-1.0 mm step along the normal (y) direction inside the boundary layer.

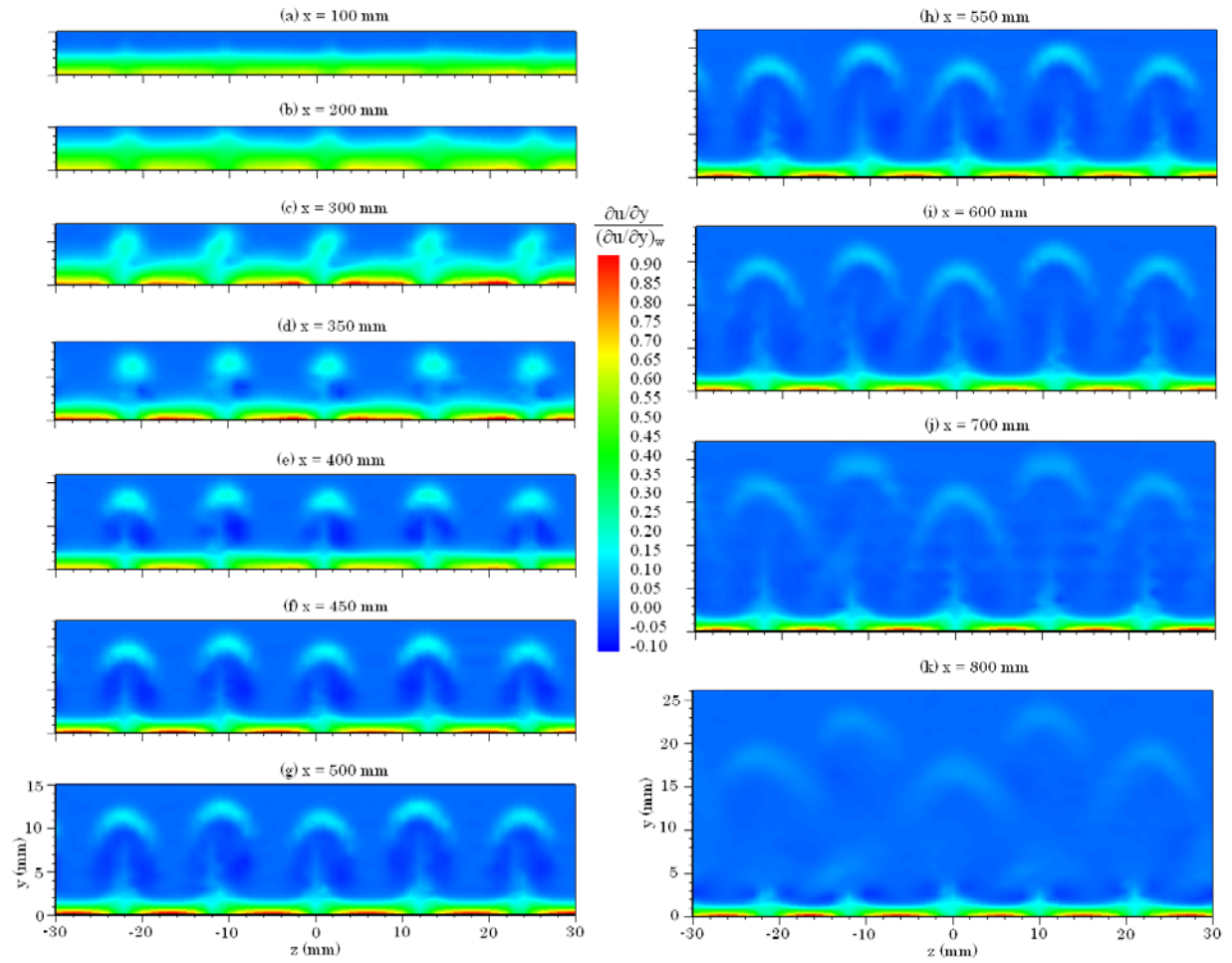

Fig. 3. Iso-shear contours of ∂u/∂y on y-z plane for several streamwise (x) locations

3. Results and Discussion

The streamwise velocities obtained from the hot-wire measurement were analyzed by using a commercial software TECPLOT. The contours of mean streamwise velocity and shear stresses (presented in term of rate of shear strains ∂u/∂y and ∂u/∂z) were then plotted in the cross-sectional (y-z) plane to show the streamwise development of Görtler vortex flow at the chosen streamwise (x) locations. They are normalized with the free-stream velocity U_∞ and the average wall shear stress.

Figure 2 shows the mean streamwise velocity (u/U_∞) contours at several streamwise (x) locations. The wavy profiles become more visible further downstream as a result of the amplification of the disturbances/vortices generated by the vertical perturbation wires placed just upstream to the concave surface leading edge. Low-momentum fluid at the upwash moves away from the surface resulting in thicker boundary layer, while high-momentum fluid at the downwash moves towards the surface resulting in thinner boundary layer. The decreasing rate of the boundary layer thickness at the downwash is lower than the increasing rate of the boundary layer thickness at the upwash, which implies that the boundary layer at downwash is more resistant to the curvature effects than that at upwash. As a result, the inflectional point observed in the velocity profiles across boundary layer first occurs at the upwash, which is the most unstable region in the boundary layer.

The wavy profiles become very prominent at x = 300 mm and develop into "horseshoe" vortices at x = 350 mm, as shown in Fig. 2(c) and (d) respectively. The appearance of the horseshoe vortices indicates that the flow is in the nonlinear region in which it is susceptible to the secondary

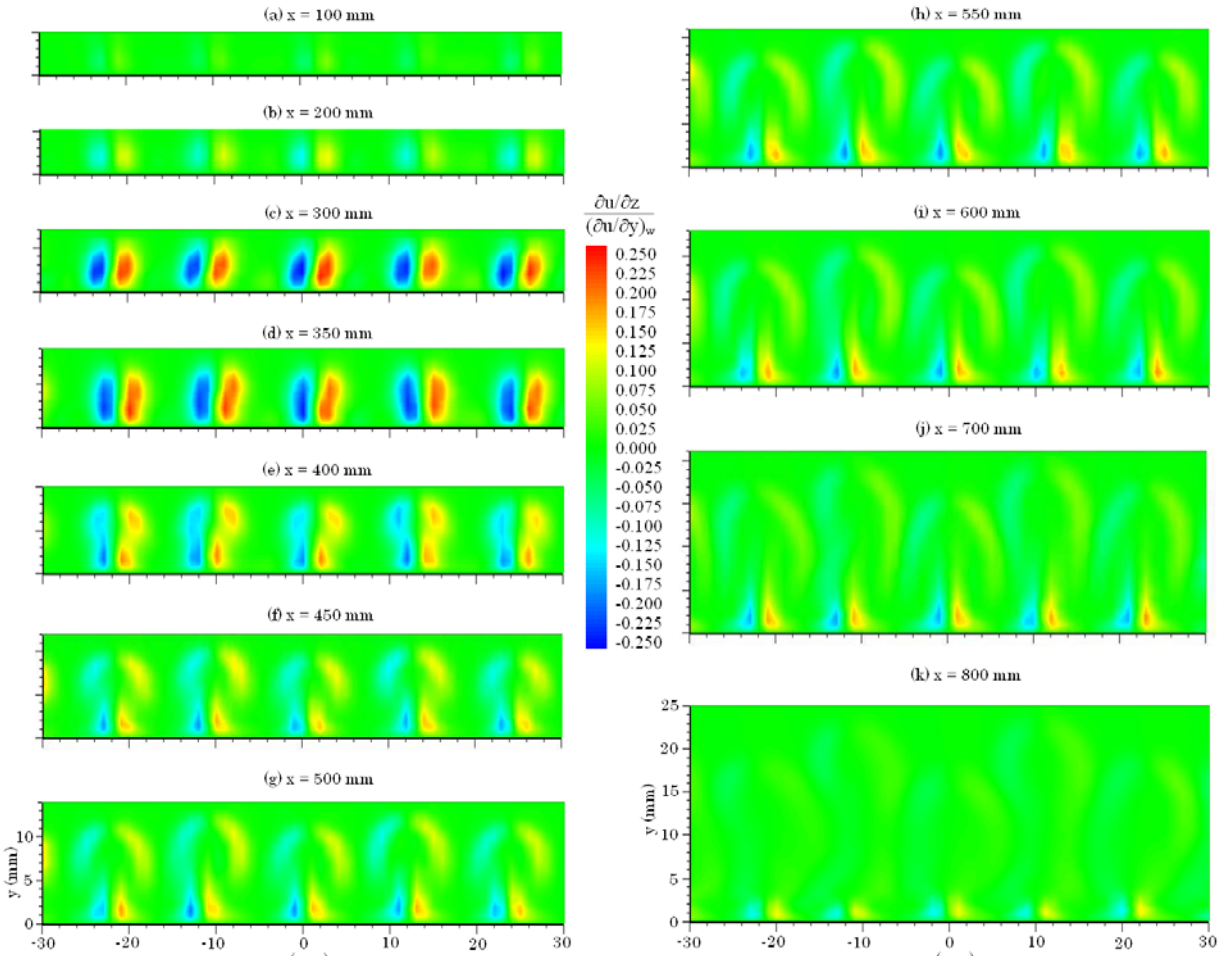

Fig. 4. Iso-shear contours of ∂u/∂z on y-z plane for several streamwise (x) locations

instability. The vortex structures are then inflected at the bottom side to form "mushroom-like" structures, as shown in Fig. 2(e) at x = 400 mm. The formation of inflection in the vortex structures indicates the formation of the inflection point in the velocity profile across the boundary layer which confirms the nonlinearity of the flow (Inagaki and Aihara, 1995). The inflection regions in the vortex structures, as well as in the velocity profile across the boundary layer, are lifted up further downstream. Consequently, the support from the stem of the vortices to the mushroom-like structures' head becomes weaker so that the vortex structures are susceptible to the free-stream flow. Finally, the vortex heads are dispersed and the flow becomes turbulent, as shown in Fig. 2(i)-(k).

The formation of the inflected velocity profiles across boundary layer was initiated from the high shear region at the upwash. Figure 3 shows the ∂u/∂y iso-shear contours at several streamwise (x) locations. In addition to the strong shear at the surface, there were other regions of strong positive shear move away from the wall, as shown in Fig. 3(c), and at x = 350 mm, two weak negative shear regions were formed below the positive high shear regions at the side of the vortex structures in Fig. 2. These strong positive and weak negative shear regions are removed from the wall in the vicinity of the low-speed streaks (Bottaro and Klingmann, 1996) as a consequence of the net upward force at the upwash. The strong positive ∂u/∂y shear region seems to correspond to the first inflection point near the boundary layer edge in the velocity profile across boundary layer, while the weak negative shear region corresponds to the second inflection point between the boundary layer edge and the concave surface. Such velocity profile suggests that the low-momentum fluid is riding above the high-momentum fluid resulting in the appearance of the "horseshoe" vortices as the secondary instability of Görtler vortices (Floryan, 1991). Yu and Liu (1994) found that these high ∂u/∂y shear layers were strongly related to the intense regions of

fluctuation and the motions of the varicose mode. Further downstream, coincidently with the decay of the mushroom-like structures, the ∂u/∂y iso-shear contours become unorganized as a result of the increased mixing due to the onset of turbulence.

In addition to the high ∂u/∂y shear regions which give rise to the inflection points in the normal direction, there are also high ∂u/∂z shear regions observed in the vicinity of the low-speed streaks, as shown in Fig. 4. In the linear region, two peaks symmetrical to the z-axis at the center of the mushroom structures are found in the contour showing the concentration of the strong positive and negative ∂u/∂z shears. The strong shear regions become more pronounced further downstream in the linear region. At x = 400 mm (Fig. 4(e)), where the flow has been in the nonlinear stage, the peaks are separated into two. The first ones are close to the wall, while the others are near the boundary layer edge, and are called "turn-over" region (Bottaro and Klingmann, 1996) in which the secondary flow turns at this point and is directed towards the wall. The appearance of these second peaks is consistent with the intense regions of fluctuation in the turbulent intensity contours which correspond to the inflectional spanwise profile of streamwise velocity. They are suspected to be responsible for the sinuous mode of secondary instability (Yu and Liu, 1991) in the form of oscillations of the low-speed streaks. Further downstream, the second peaks near the boundary layer edge decay as the mushroom-like structures collapse prior to turbulence. At the same time, the first peaks close to the wall become less pronounced indicating that the high shear regions decay and finally vanish as the flow becomes fully turbulent.

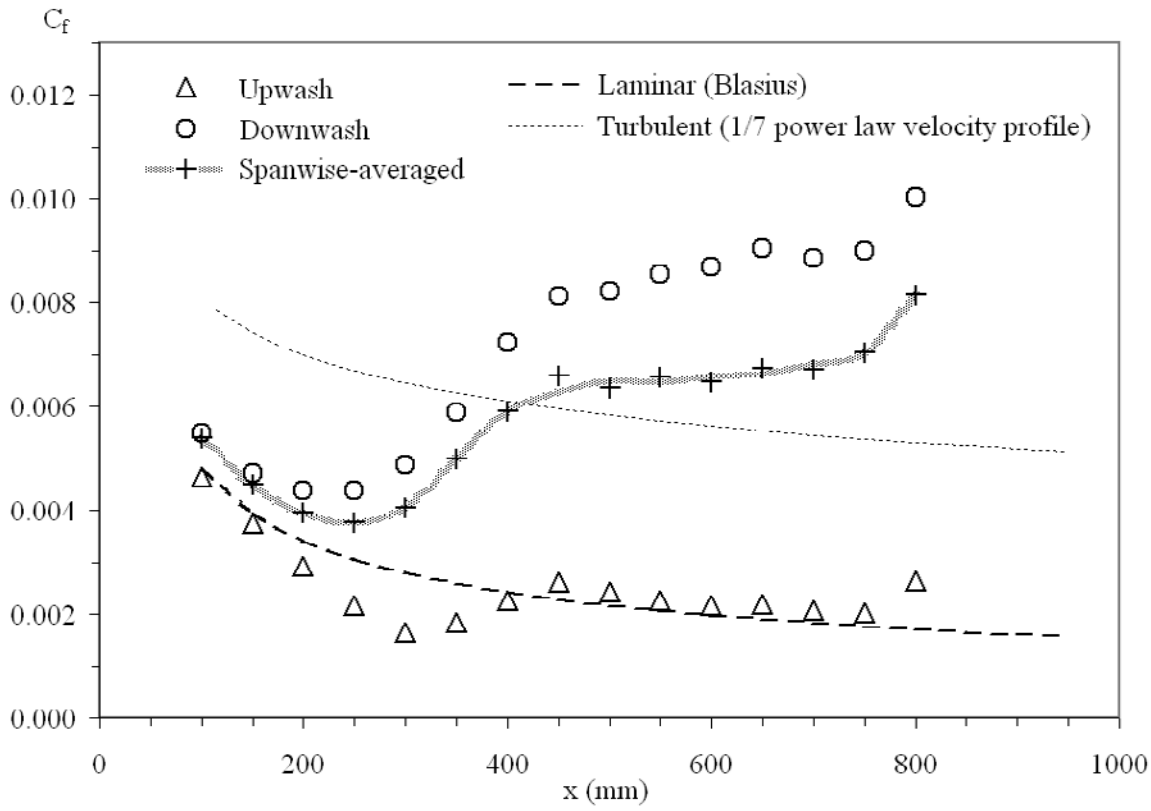

Fig. 5. Streamwise development of wall shear stress coefficient (C_f)

The developments of the wall shear stress in term of its coefficient C_f at upwash and downwash in the streamwise direction, and their spanwise-averaged values, are shown in Fig. 5. The wall shear stress was estimated based on the velocity gradient of the "linear" region across the boundary layer. An error analysis was then carried out to obtain the standard error of the wall shear stress estimates. The maximum standard error for the present case (λ_m = 12 mm, U_∞ = 2.85 m/s) was found to be 2.3%. The wall shear stress curves for Blasius laminar boundary layer flow and for low Reynolds number turbulent boundary layer flow on a flat plate are also shown in the figure for comparison. The turbulent curve was obtained from the Blasius solution for turbulent

boundary layer on smooth surface and one-seventh power law turbulent boundary layer velocity profile, that is $C_f = 0.0576/Re_x^{1/5}$.

As shown in Fig. 5, the wall shear stress at the upwash initially decreases at a rate higher than the Blasius curve until it reaches a minimum at x = 300 mm. The wall shear stress at the minimum point is 59% of the Blasius value at that position. After reaching its minimum point, the wall shear stress begins to increase downstream to reach and follow the Blasius curve until the decay of the mushroom-like structures at x = 750 mm. This finding is consistent with the numerical results of Bottaro and Klingmann (1996) who found that the nonlinear development of the Görtler instability leads to an initial decrease of the wall shear stress at the upwash prior to the subsequent slight increase due to the secondary instability.

At downwash region, the wall shear stress also initially decreases downstream, but at the rate slightly lower than the Blasius curve. However, at x = 250 mm, it starts to increase considerably downstream until x = 450 mm where the increasing rate reduces abruptly. A significant increase of the wall shear stress occurs again at x = 750 mm as a result of the increased mixing due to the onset of turbulence. This is confirmed by the increase of the turbulence intensity near the wall, as reported by Tandiono et al. (2008). As shown in Fig. 5, the spanwise-averaged curve is closer to the downwash curve than to the upwash curve. This implies that the spanwise distribution of wall shear stress is such that it is wider and flatter at downwash region than at upwash region, especially at the upstream locations.

From the leading edge to x = 200 mm, the spanwise-averaged wall shear stress curve lies slightly above the Blasius curve, as shown in Fig. 5, but it decreases at the same rate as the Blasius curve. At x = 250 mm, the spanwise-averaged curve starts to depart from the Blasius curve indicating that the instability has grown nonlinearly. The wall shear stress subsequently increases well beyond the turbulent curve for flat plate boundary layer. Computational studies of Sabry and Liu (1991) showed that the further enhancement of the wall shear stress was due to the effect of the nonlinear steady longitudinal Görtler vortices. In the absence of the secondary instability, the spanwise-averaged wall shear stress appeared to bridge the Blasius curve and the flat plate turbulent boundary layer curve. The presence of the secondary instability seemed to further increase the wall shear stress well beyond the turbulent values (Girgis and Liu 2006).

4. Conclusions

The development of shear stress in Görtler vortex flow has been experimentally investigated on concave surface of 1.0 m radius of curvature. To obtain uniform wavelengths, the Görtler vortices were pre-set by thin vertical wires of 0.2 mm diameter placed 10 mm upstream and perpendicular to the concave surface leading edge. Mean streamwise velocity and shear stress developments in the flow field were visualized from the mean velocity data obtained by the hot-wire measurement.

Since the spacing of the disturbances wires corresponds to the most amplified wavelength Görtler vortices, the wavelength of the vortices are preserved downstream which confirms the prediction of the most amplified wavelength Görtler vortices. The wavy profiles induced by the perturbation wires were amplified downstream to form horseshoe vortices and subsequently mushroom-like structures in the nonlinear region as the result of the onset of secondary instability. The high $\partial u/\partial y$ regions are found to be related to the inflectional velocity profile across boundary layer which is responsible for the varicose mode of secondary instability. Furthermore, the high $\partial u/\partial z$ shear regions are correlated to the inflectional velocity profile along spanwise which is responsible for the sinuous mode of secondary instability.

Compared to the wall shear stress of the Blasius solution for flat plate boundary layer, the linear development of Görtler vortices gives rise to a lower wall shear stress at upwash and a higher wall shear stress at downwash. The enhancement of the wall shear stress is due to the effect of nonlinear development of Görtler vortices. The presence of the secondary instability further increases the wall shear stress well beyond the turbulent values.

References

Ajakh, A., Kestoras, M. D., Toe, R., and Peerhossaini, H., Influence of forced perturbations in the stagnation region on Görtler instability, AIAA Journal, 37-12 (1999), 1572-1577.

Bippes, H. and Görtler, H., Three-dimensional disturbances in the boundary layer along a concave wall, Acta Mechanica, 14-4 (1972), 251-267.

Bottaro, A. and Klingmann, B. G. B., On the linear breakdown of Görtler vortices, European Journal of Mechanics, B/Fluids, 15-3 (1996), 301-330.

Floryan, J. M., On the Görtler instability of boundary layers Progress in Aerospace Sciences, 28-3 (1991), 235-271.

Girgis, I. G. and Liu, J. T. C., Nonlinear mechanics of wavy instability of steady longitudinal vortices and its effect on skin friction rise in boundary layer flow, Physics of Fluids, 18-2 (2006), 024102-024112.

Görtler, H., Über eine dreidimensionale Instabilität laminarer Grenzschichten an konkaven Wänden, Gesellschaft der Wissenschaften zu Göttingen, Nachrichten, Mathematik, 2-1 (1940), 32p. Translated: On the three-dimensional instability of laminar boundary layers on concave walls, NACA TM 1375 (1954).

Hall, P. and Horseman, N. J., Linear inviscid secondary instability of longitudinal vortex structures in boundary layers, Journal of Fluid Mechanics, 232 (1991), 357-375.

Inagaki, K. and Alhara, Y., An experimental study of the transition region of the boundary layer along a concave wall, European Journal of Mechanics, B/Fluids, 14-2 (1995), 143-168.

Luchini, P. and Bottaro, A., Görtler vortices: a backward-in-time approach to the receptivity problem, Journal of Fluid Mechanics, 363 (1998), 1-23.

Mitsudharmadi, H., Winoto, S. H., and Shah, D. A., Development of boundary layer flow in the presence of forced wavelength Görtler vortices, Physics of Fluids, 16-11 (2004), 3983-3996.

Peerhossaini, H. and Bahri, F., On the spectral distribution of the modes in nonlinear Görtler instability, Experimental Thermal and Fluid Science, 16-3 (1998), 195-208.

Petitjeans, P., Aider, J. L., and Wesfreid, J. E., Mass and momentum transport in longitudinal vortical structures in liquid flow:example of Goertler vortices, Experiments in Fluids, 23-5 (1997), 388-394.

Sabry, A. S. and Liu, J. T. C., Longitudinal vorticity elements in boundary layers. Nonlinear development from initial Goertler vortices as a prototype problem, Journal of Fluid Mechanics, 231 (1991), 615-663.

Swearingen, J. D. and Blackwelder, R. F., Growth and breakdown of streamwise vortices in the presence of a wall, Journal of Fluid Mechanics, 182 (1987), 255-290.

Tandiono, Winoto, S. H., and Shah, D. A., Linear and nonlinear development of Görtler vortices, Physics of Fluids, 20-9 (2008), 094103.

Winoto, S. H. and Crane, R. I., Vortex structure in laminar boundary layers on a concave wall, International Journal of Heat and Fluid Flow, 2-4 (1980), 221-231.

Winoto, S. H., Mitsudharmadi, H., and Shah, D. A., Visualizing Görtler vortices, Journal of Visualization, 8-4 (2005), 315-322.

Wortmann, F. X., Visualization of transition, Journal of Fluid Mechanics, 38 (1969), 473-483.

Yu, X. and Liu, J. T. C., The secondary instability of Görtler flow, Physics of Fluids A, 3-8 (1991), 1845-1847.

Yu, X. and Liu, J. T. C., On the mechanism of sinuous and varicose modes in three-dimensional viscous secondary instability of nonlinear Görtler rolls, Physics of Fluids, 6-2 (1994), 736-750.

Author Profile

Tandiono: He is currently a PhD Research Scholar at the Department of Mechanical Engineering, National University of Singapore. He received his B. Eng degree in Mechanical Engineering from Institut Teknologi Bandung, Bandung, Indonesia in 2004, and was awarded the best graduate in the Department of Mechanical Engineering, Institut Teknologi Bandung. His research interests are in boundary layer flows and hot-wire anemometry.

S. H. Winoto: He obtained his PhD from Imperial College, London in 1980 and joined the National University of Singapore in the same year. His research interests include boundary layer flows, jet flows and their applications, and fluid machinery. He was awarded the American Society of Mechanical Engineers (ASME) Region XIII Award in 2001 and the Journal of Visualization Award of Japan in 2007.

D. A. Shah: He obtained his Master of Engineering from Indian Institute of Science, Bangalore, India in 1980 and PhD from University of Newcastle, Australia in 1988. He spent about a year as a faculty member at the Indian Institute of Technology, Kunpur, India before joining the National University of Singapore in 1989. He has been involved in organizing some international conferences in Singapore. He is a member of the American Society and Mechanical Engineers (ASME) and served on a number of Committees in the ASME Singapore Section. His research interests include hot-wire anemometry, turbulent shear flows, bluff bodies, and industrial aerodynamics.